

**TO:** Texas Air Research Center (or Texas Hazardous Waste Research Center)

**FROM:** Investigators Zhanhu Guo, Suying Wei  
Institution Lamar University  
Contact Information zhanhu.guo@lamar.edu

**SUBJECT:** Final Report

**PROJECT NUMBER:**

**PROJECT TITLE: Novel Adsorbents: Carbon Nanocomposites towards Toxic Cr(VI) Removal**

**PROJECT PERIOD: 09/2013 ~ 05/2015**

**DATE: 02/05/2016**

**Up to 5 pages of progress report including the following sections:**

### **Project Description**

The explicit purpose of this project is to chart a new direction for our research: grow functional nano-adsorbents on cellulose substrates and to use these materials in filtration column units for continuous, fast and complete Cr(VI) removal. The magnetic carbon nanocomposite adsorbents, consisting of iron or iron oxide nanoparticles coated with carbon shell, will be fabricated using the solution mixing cellulose and iron precursors and subsequent thermal annealing method developed by the PIs. The nanocomposite magnetic carbon core-shell nano- adsorbents packing length, density and assembling configuration in the filtration column as well as flow rate and circulation time of polluted water will be systematically studied by using real industry polluted water. The iron@carbon core-shell nanoparticles are expected to enlarge the Cr(VI) removal efficiency and capability. In particular, the Cr(VI) removal under low PH value environment is realized using the as-obtained anti-corrosive iron@carbon core-shell nano-adsorbents. The Cr(VI) removal mechanisms will be exploited by studying the Cr valence state change on the carbon nanocomposites surface with X-ray photoelectron spectroscopy and magnetization change before and after treatment.

### **Objectives**

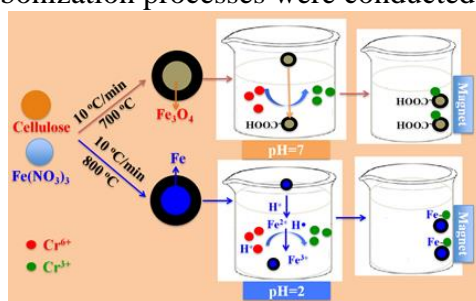
The objective of this project is to (1) develop facile and cost effective processes to manufacture magnetic carbon nanocomposites; (2) investigate the Cr(VI) removal from polluted water by the created magnetic carbon nanocomposites in a filtration column system; (3) determine the Cr(VI) removal mechanisms. In this report, the magnetic carbon nanocomposites were synthesized and

their performances on Cr(VI) removal from polluted solution were investigated. Meanwhile, the mechanisms involved in the Cr(VI) removal processes were discussed.

## Methodology

### Synthesis of magnetic carbon nanocomposite fabrics

Three major steps were involved for the synthesis of magnetic carbon nanocomposites. First, 20.0 g of  $\text{Fe}(\text{NO}_3)_3 \cdot 9\text{H}_2\text{O}$  was dissolved in 200 mL of ethanol, and was mechanically stirred for 30 min. 2.0 g of cellulose was then mixed with the  $\text{Fe}(\text{NO}_3)_3$  solution, and was stirred continuously for another 2 h, in order to make  $\text{Fe}^{3+}$  homogeneously distributed in cellulose. Second, the mixtures were kept at room temperature for complete evaporation of ethanol. The remaining solid samples were then calcined at different annealing temperatures (600, 700, and 800 °C), different heating rates (2, 5 and 10 °C/min), and retention times (0, 30 and 60 min). The samples were named as MC a–b–c, and the “a”, “b” and “c” were the carbonization temperature, heating rate and retention time, respectively. All the carbonization processes were conducted in nitrogen atmosphere.



**Scheme 1.** Magnetic carbon nano-adsorbents fabricated by using cellulose and  $\text{Fe}(\text{NO}_3)_3$  as the carbon and iron precursors have demonstrated great Cr(VI) removal performance: High annealing temperature, i.e., 800 °C, can result in metallic iron @ carbon core-shell magnetic nanoparticles with highest Cr(VI) removal capacity ( $278.8 \text{ mg g}^{-1}$ ) in acidic solutions. While iron oxide @ carbon core-shell magnetic nanoparticles is produced under carbonization temperature of 700 °C, and it has good Cr(VI) capacity ( $22.8 \text{ mg g}^{-1}$ ) in neutral solutions due to its larger specific surface area ( $247.14 \text{ m}^2 \text{ g}^{-1}$ ).

## Accomplishments/Problems

### 1. Characterizations

The SEM images of the magnetic carbons (Fig. 1) show that the particle becomes smaller and more uniform with increasing the carbonization temperature. The irregular magnetic carbon nanoparticles were observed with a carbonization temperature of 600 °C (Fig. 1A), while uniform spherical particles with an average diameter of  $\sim 80 \text{ nm}$  (Fig. 1C) were obtained at a carbonization temperature of 800 °C. The iron formed in the magnetic carbons fabricated at different carbonization temperatures were investigated by XRD (Fig. 2A). The diffraction peaks at  $30.1^\circ$ ,  $35.5^\circ$ ,  $56.9^\circ$  and  $62.6^\circ$  correspond to the (220), (311), (511) and (440) reflections of  $\text{Fe}_3\text{O}_4$  (Fig. 2A (a&b)), respectively. The diffractions peaks at  $25.6^\circ$ ,  $44.7^\circ$  and  $45.0^\circ$  are indexed as the (002), (100) and (110) planes of the cubic Fe, zero valence iron (ZVI). The high intensity ratio of  $\text{Fe}_3\text{O}_4$  to ZVI in MC6-10 and MC7-10 shows that  $\text{Fe}^{3+}$  has been transformed to  $\text{Fe}_3\text{O}_4$  rather than been reduced to ZVI with the carbonization temperatures of 600 and 700 °C. However, the ZVI peaks with high intensity in the MC8 indicate that most  $\text{Fe}^{3+}$  has been reduced to ZVI by the carbon at 800 °C.

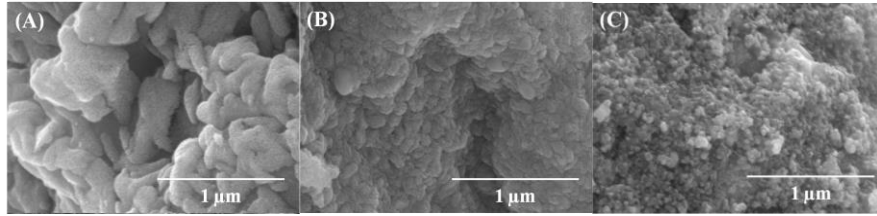


**Fig. 1** SEM images of magnetic carbons: (A) MC6-10, (B) MC7-10 and (C) MC8-10.

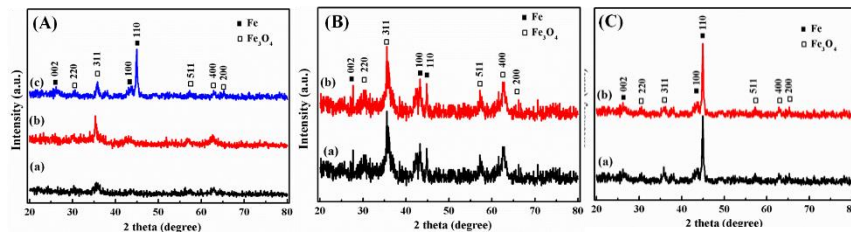


**Fig. 2** XRD patterns of magnetic carbons synthesized (A) with a carbonization temperature of (a) 600, (b) 700 and (c) 800 °C (heating rate: 10 °C/min); (B) with a heating rate of (a) 2 and (b) 5 °C/min (final temperature: 800 °C); and (C) with a retention time of (a) 30 and (b) 60 min (heating rate: 10 °C/min, final temperature: 800 °C).

## 2. Cr(VI) removal

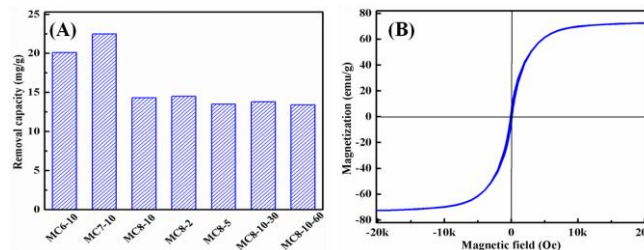


**Fig. 3** (A) Cr(VI) removal by the synthesized magnetic carbons with an initial pH of 7.0; (B) magnetic hysteresis loop of the MC8-10 after being treated with Cr(VI).

As shown in Fig. 3A, MC7-10 was observed to exhibit the highest adsorption capacity of 22.8 mg/g in the neutral solution, followed by the MC6-10 (20.0 mg/g). No obvious difference in the adsorption capacity was observed for the magnetic carbons synthesized with different heating rates. However, the adsorption capacity decreased with increasing the retention time. The MC8-10-60 has the lowest adsorption capacity of 10.2 mg/g. These are consistent with the results of their specific surface area. The largest specific surface area of MC7-10 (247.14 m<sup>2</sup>/g) contributes to the highest Cr(VI) adsorption capacity. While the decreased specific surface area with increasing the retention time results in the decreased Cr(VI) adsorption capacity. The removal capacity of MC7-10 is much higher than the pristine cellulose (4.1 mg/g), active carbon (5.2 mg/g), magnetic carbon derived from cotton fabrics (3.73 mg/g), and the nitrogen doped magnetic carbon derived from rice husk (15.6 mg/g). Here, the MC7-10 was taken as an example to disclose the Cr(VI) removal mechanisms in neutral solution. The synthesized MC7-10 exhibits a good magnetic property with a saturation magnetization of 72.2 emu/g, and no obvious decreased magnetization was observed after being treated with the Cr(VI) solution at pH 7.0 (Fig. 3B), indicating that the carbon layer is stable and protects the Fe<sub>3</sub>O<sub>4</sub> against dissolving in the solution.

It also shows that the  $\text{Fe}_3\text{O}_4$  in the magnetic carbon doesn't participate in the Cr(VI) removal process. The  $\text{Fe}_3\text{O}_4$  particles in the adsorbent just act as the magnetic core, leading to the easy separation of adsorbent from solutions after being treated with Cr(VI). The larger specific surface area of the MC7-10 facilitates the Cr(VI) iron adsorption, indicating that the Cr(VI) removal was mainly contributed by the carbon layer.

The pH value has been demonstrated important for the Cr(VI) removal by magnetic carbons. The Cr(VI) removal capacities of the synthesized magnetic carbons were also determined with an initial pH of 2.0. As shown in Fig. 4A, the greatest Cr(VI) removal capacity of 278.8 mg/g was observed for MC8-10, a little higher than that of MC8-10-30 and MC8-10-60, and much higher than that of the MC6-10, MC7-10, MC8-5 and MC8-2. This indicates that the Cr(VI) removal by the magnetic carbon in acidic solution is highly dependent on the ZVI in the magnetic carbon. However, the removal capacity is also much higher than that of ZVI/chitosan (55.8 mg/g), ZVI/ $\text{Fe}_3\text{O}_4$  nanoparticles (186.3 mg/g), and iron doped ordered mesoporous carbon (256.8 mg/g).

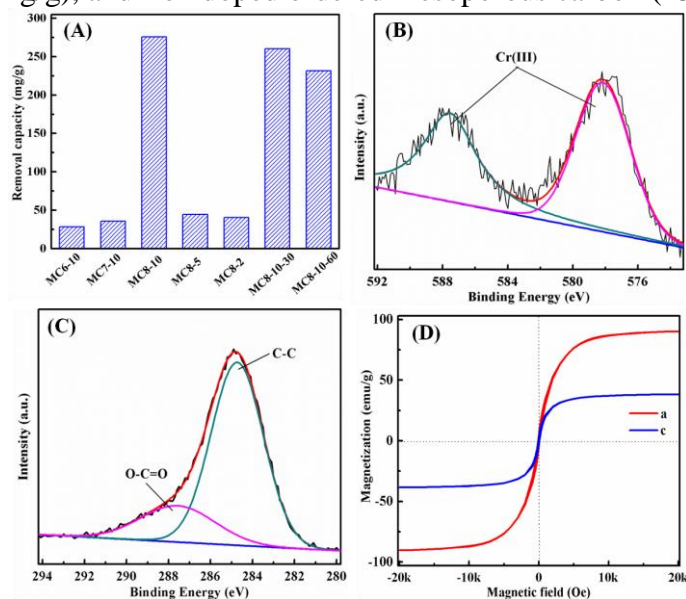


**Fig. 4** (A) Cr(VI) removal by the synthesized magnetic carbons with an initial solution pH of 2.0; (B) Cr2p and (C) C1s XPS spectra of MC8-10 after being treated with Cr(VI) solution; (D) magnetic hysteresis loop of the MC8-10 (a) before and (b) after being treated with Cr(VI).

It is interesting that the Cr(VI) removal capacities of the magnetic carbons synthesized with a final carbonization temperature of 800 °C and a heating rate of 10 °C/min (MC8-10, MC8-10-30 and MC8-10-60) are several times higher than these of the others synthesized in this study. It indicates that the ZVI in the magnetic carbons plays an important role in the Cr(VI) removal from acidic solution. Moreover, the magnetic carbons with  $\text{Fe}_3\text{O}_4$  core, including MC6-10, MC7-10, MC8-5 and MC8-2, have higher removal capacities in the acidic solution than in the neutral solution (Fig. 3A). As documented, the most important forms of Cr(VI) in aqueous solution are chromate ( $\text{CrO}_4^{2-}$ ), dichromate ( $\text{Cr}_2\text{O}_7^{2-}$ ) and hydrogen chromate ( $\text{HCrO}_4^-$  and  $\text{H}_2\text{CrO}_4$ ) and these ion forms are related to the solution pH. The  $\text{HCrO}_4^-$  is the dominant form when pH is lower than 6.8, while only  $\text{CrO}_4^{2-}$  is stable when pH is above 6.8. The  $\text{HCrO}_4^-$  with a higher redox potential (1.33 V) can be easily reduced to Cr(III) by the carbon layer. The MC8-10 has a higher capacity than MC8-10-30 and MC8-10-60 mainly due to its bigger specific surface area. The MC8-10 was taken as an

example to disclose the mechanisms involved in the Cr(VI) in acidic solution. Fig. 4B shows the Cr2p spectra of the MC8-10 after being treated by 2.0 g/L Cr(VI) solution with an initial pH of 2.0 for 30 min. The binding energy peaks at 578.1 and 587.5 eV indicate that the adsorbed chromium was in the form of Cr(III). No Cr(VI) was detected on the surface of MC8-10, indicating that the Cr(VI) was completely reduced to Cr(III). Fig. 4C shows the C1s XPS spectrum of the MC8-10 after being treated with Cr(VI). The observed two energy peaks at 284.7 and 288.2 eV are related to the C-C and O-C=O. The newly generated O-C=O group indicates the oxidation of carbon by Cr(VI), compared to the C1s spectrum of the synthesized MC8-10. Meanwhile, the magnetic property of MC-10 before and after being treated with Cr(VI) was measured (Fig. 4D). It shows that the MC8-10 exhibits a good magnetic property with a saturation magnetization of 90.2 emu/g, and a sharp decrease (38.4 emu/g) was observed after being treated with an initial pH of 2.0 for 30 min, indicating that the ZVI has been consumed for the Cr(VI) removal.

### 3. Cr(VI) removal mechanisms

The ZVI was dissolved by acidic solution and produced the reductive intermediates such as H<sup>•</sup>, hydrogen and Fe<sup>2+</sup>, which act as electron donors for the reduction of Cr(VI) to Cr(III). The ZVI was consumed for the Cr(VI) reduction and formed precipitants of iron and chromium hydroxides on the adsorbents surface, leading to the decreased magnetization. However, the magnetic carbons also exhibit a large magnetization even though they are treated with acid solutions, which can be easily separated by a permanent magnet from the solutions after being treated with Cr(VI). ZVI has been demonstrated much great Cr(VI) removal than Fe<sub>3</sub>O<sub>4</sub> and Fe<sub>2</sub>O<sub>3</sub> since the ZVI can provide more electrons for the Cr(VI) reduction in the acidic solution. Generally, the reduction of Cr(VI) to Cr(III) by the oxidation of ZVI as well as the carbon layer of the magnetic carbon was determined to be the main mechanism of Cr(VI) removal by the magnetic carbons in the acidic solution.

### Future Work

The metallic iron @ carbon core-shell magnetic nanoparticles with highest Cr(VI) removal capacity (278.8 mg g<sup>-1</sup>) is more competitive compared with other magnetic composite nano-adsorbents. A continuous flow system packed with the carbon nanocomposites will be setup and used to filtrate the Cr(VI)-containing wastewater. The fluid flow rate, residence time, removal rate and percentage, polluted water treatment capacity will be determined.

### List of Publications and Presentations

1. Polyaniline Coated Ethyl Cellulose with Improved Hexavalent Chromium Removal; B. Qiu, C. Xu, D. Sun, H. Yi, J. Guo, X. Zhang, H. Qu, M. Guerrero, X. Wang, N. Noel, Z. Luo, Z. Guo & S. Wei, *ACS Sustainable Chemistry & Engineering*, 2(8), 2070-2080 (2014)
2. Polyethylenimine Facilitated Ethyl Cellulose for Hexavalent Chromium Removal with a Wide pH Range; B. Qiu, J. Guo, X. Zhang, D. Sun, H. Gu, Q. Wang, H. Wang, X. Wang, X. Zhang, B. L. Weeks, Z. Guo, & S. Wei; *ACS Applied Materials & Interfaces*, 6, 19816-19824 (2014)
3. Cr(VI) removal by magnetic carbon nanocomposites derived from cellulose at different carbonization temperatures; B. Qiu, Y. Wang, D. Sun, Q. Wang, X. Zhang, B. L. Weeks, R. O'Connor, X. Huang, S. Wei & Z. Guo, *Journal of Materials Chemistry A*, 3, 9817-9825 (2015)